https://doi.org/10.5194/bg-2020-230
Preprint. Discussion started: 2 July 2020

Biogeosciences Discussions

Sub-soil irrigation does not lower greenhouse gas emission from drained peat meadows

Stefan Theodorus Johannes Weideveld[1*], Weier Liu[2], Merit van den Berg[1], Leon Peter Maria Lamers[1], Christian Fritz[1],

[1] - Aquatic Ecology and Environmental Biology, Institute for Water and Wetland Research, Radboud University, Heyendaalseweg 135, 6525, AJ, Nijmegen, the Netherlands.

[2] - Integrated Research on Energy, Environment and Society, University of Groningen, Nijenborgh 6, 9747 AG, Groningen, the Netherlands

*Corresponding author

E-mail addresses: *S.Weideveld@science.ru.nl, Stefan.Weideveld1@gmail.com (S.T.J. Weideveld)*

Abstract

Current water management in drained peatlands to facilitate agricultural use, leads to soil subsidence and strongly increases greenhouse gas (GHG) emission. High-density, sub-soil irrigation/drainage systems have been proposed as a potential climate mitigation measure, while maintaining high biomass production. In summer, sub-soil irrigation can potentially reduce peat decomposition by preventing groundwater tables to drop below -60 cm.

In 2017-2018, we evaluated the effects of sub-soil irrigation on GHG emissions (CO_2, CH_4, N_2O) for four dairy farms on drained peat meadows in the Netherlands. Each farm had a treatment site with perforated pipes at 70 cm below soil level spacing 5-6 m to improve both drainage (winter- spring) and irrigation (summer) of the subsoil, and a control site drained only by ditches (ditch water level -60/-90 cm, 100 m distance between ditches). GHG emissions were measured using closed chambers (0.8 x 0.8 m) every 2-4 weeks. C inputs by manure and C export by grass yields were accounted for.

Unexpectedly, sub-soil irrigation hardly affected ecosystem respiration (R_{eco}) despite raising summer groundwater tables (GWT) by 6-18 cm, and even up to 50 cm during drought. Only when the groundwater table of sub-soil irrigation sites was substantially higher than the control value (> 20 cm), R_{eco} was significantly lower ($p<0.01$), indicating a small effect of

https://doi.org/10.5194/bg-2020-230
Preprint. Discussion started: 2 July 2020


Biogeosciences Discussions Open Access EGU

irrigation on C turnover. During wet conditions sub-soil pipes lowered water levels by 1-20 cm, without a significant effect on R_{eco}. As a result, R_{eco} differed little (>3%) between sub-soil irrigation and control sites on an annual base.

CO_2 fluxes were high at all locations, exceeding 45 t CO_2 ha^{-1} a^{-1}, even where peat was covered by clay (25-40 cm). Despite extended drought episodes and lower water levels in 2018, we found lower annual CO_2 fluxes than in 2017 indicating drought stress for microbial respiration. Contrary to our expectation, there was no difference between the yearly greenhouse balance of the sub-soil irrigated (64 t CO_2–eq ha^{-1} yr^{-1} in 2017, 53 in 2018) and control sites (61 t CO_2–eq ha^{-1} yr^{-1} in 2017, 51 in 2018). Emissions of N_2O were lower (3±1 t CO_2–eq ha^{-1} yr^{-1}) in 2017 than in 2018 (5±2 t CO_2–eq ha^{-1} yr^{-1}), without treatment effects. The contribution of CH_4 to the total GHG budget was negligible (<0.1%), with lower GWT favoring CH_4 oxidation over its production. Even during the 2018 drought, sub-soil irrigation had only little effect on yields (9.7 vs. 9.1 t DM ha^{-1} yr^{-1}), suggesting that increased GWT failed to increase plant water supply. This indicates that peat oxidation is hardly affected, probably because GWT increase only takes place in deeper soil layers (60-120 cm depth).

We conclude that, although our field-scale experimental research revealed substantial differences in summer GWT and timing/intensity of irrigation and drainage, sub-soil irrigation fails to lower annual GHG emission and is unsuitable as a climate mitigation strategy. Future research should focus on potential effects of GWT manipulation in the uppermost organic layers (-30 cm and higher) on GHG emissions from drained peatlands.

1 Introduction

Peatlands cover only 3% of the land and freshwater surface of the planet, yet they contain one third of the total carbon (C) stored in soils (Joosten and Clarke, 2002). Natural peatlands capture C by producing more organic material than is decomposed due to waterlogged conditions (Gorham et al., 2012;Lamers et al., 2015). Drainage of peatlands for agricultural purposes leads to aerobic oxidation of organic material resulting in soil subsidence and the concomitant release of CO_2 and N_2O (Regina et al., 2004;Joosten, 2009;Hoogland et al., 2012;Lamers et al., 2015;Leifeld and Menichetti, 2018). Soil subsidence occurs when the groundwater table (GWT) drops through drainage, leading to physical and chemical changes of the peat. This results in consolidation, shrinkage, compaction and increased decomposition (Stephens et al., 1984;Hooijer et al., 2010). Soil subsidence increases the risk of flooding (frequency and duration) in areas where soil surface subsides below river and sea levels (Syvitski

https://doi.org/10.5194/bg-2020-230
Preprint. Discussion started: 2 July 2020

et al., 2009). In the Netherlands, 26% of the surface area is currently below sea level, an area currently inhabited by 4 million people (Kabat et al., 2009). This area is expected to increase due to further land subsidence, while sea level is rising at the same time, which is a general issue of coastal peatlands (Erkens et al., 2016). Additionally, peatland subsidence alters hydrology, leading to drainage problems, salt water intrusion and loss of productive land (Dawson et al., 2010;Herbert et al., 2015). This will result in strongly increased societal costs and difficulties in maintaining productive land use (Van den Born et al., 2016;Tiggeloven et al., 2020).

The peatland area used for agriculture is estimated at 10% for the USA and 15% Canada, and varies from less than 5 to more than 80% or Europe (Lamers et al., 2015). In the Netherlands, 85% of the peatland areas are in agricultural use (Tanneberger et al., 2017), leading to CO_2 emissions of 7 Mt CO_2-eq per year, amounting to 4% of total national greenhouse gas (GHG) emissions (Couwenberg, 2009). Fundamental changes in the management of peatlands are required if land use, biodiversity and socio-economic values including GHG emission reduction are to be maintained. A higher groundwater table (GWT) creates anaerobic conditions (Berglund and Berglund, 2011b), which could lower peat oxidation rates and therefore CO_2 emissions and soil subsidence (Van den Bos and van de Plassche, 2003;Lloyd, 2006b;Wilson et al., 2016b;Van Huissteden et al., 2006).

To reduce peat oxidation, drastic rewetting (raising the water table to -20 cm below soil surface or higher) would be the ideal option (Hendriks et al., 2007a;Jurasinski et al., 2016). However, current agricultural use would then no longer be feasible. Therefore, there is a incentive to explore options where the effects of peat oxidation are mitigated but land use is not changed. A solution suggested to reduce C loss and land subsidence, which is already in use in the Netherlands, is sub-soil irrigation (SSI). The aim of this management option is to raise the GWT during summer when CO_2 emissions are highest due to high temperatures in concert with low GWT. Raising the GWT in the summer could prove effective to limit aerobic peat oxidation (Hoving et al., 2015;Kechavarzi et al., 2007). Irrigation pipes are placed in the soil at a depth of 70 cm below the soil surface, and 10 cm below ditchwater level. This will have two effects: drainage when there is excess water (mostly in autumn, winter and spring), and irrigation in dry periods (summer). This will force the GWT towards the ditch water level at around -60 cm

https://doi.org/10.5194/bg-2020-230
Preprint. Discussion started: 2 July 2020

below the soil surface. The drainage effect results in more of the peat being exposed to oxygen, but since this happens in a colder period, it is expected that the effect of irrigation on CO_2 emissions during summer will be much larger. There are, however, few comprehensive studies that report on the effect of sub-soil irrigation on total GHG emissions and C balances for peat soils (Van den Akker et al., 2010;Hendriks et al., 2007b). The hypothesis for the effectiveness of SSI is based on the assumption that peat layers below -70 cm contribute most to GHG emissions. However, this is only based on soil subsidence data, and until now there have not been any studies that directly measured GHG fluxes to test the expected GHG reduction.

The aim of our study was therefore to quantify the effect of sub-soil irrigation as an alternative drainage technique on the GWT and the GHG balance. The main research questions were whether, compared to traditional drainage, sub-soil irrigation of peat meadows can 1) achieve the intended regulation of GWT within each year and between years (i.e. irrigation during summer and drainage during winter), and 2) lead to a significant reduction of peat oxidation and GHG emission?

2 Material and methods

2.1 Study area

The study areas are located in a peat meadow area in the province of Friesland, the Netherlands. The climate is humid Atlantic with an average annual precipitation of 840 mm and an average annual temperature of 10.1°C (KNMI, reference period 1999-2018).

About 62% of the Frisian peatland region is now used as grassland for dairy farming (Hartman et al., 2012). Agricultural land in Friesland is farmed intensively, with high yields, and intensive fertilization (>230 kg N ha^{-1} yr^{-1}). It is characterized by large fields with deep drainage, as one third of the fields are drained to -90 – -120 cm below soil surface. Large parts of these grasslands are covered with a carbon rich clay layer, ranging from 20–40 cm thick. The peat layer below has a thickness of 80–200 cm, which consists of sphagnum peat on top of sedge, reed and alder peat. The top 30 cm of the peat layer is strongly humified (van Post H8-H10) and the peat below 60 – 70 cm deep is only moderately decomposed (van Post H5-H7). On two locations (C and D, see below), there is a 'schalter' peat layer present, highly laminated peat (compacted/ hydrophobic layers of *Sphagnum cuspidatum* remnants) with poor degradability and poor water permeability. The grasslands are dominated by

https://doi.org/10.5194/bg-2020-230
Preprint. Discussion started: 2 July 2020

Lolium Perenne; other species such as *Holcus lanatus, Elytrigia repens, Ranoculus acris* and *Trivolium repens* are present in a low abundance.

Table 1 Soil and land use characteristics of the research sites in the peat meadows of Friesland, the Netherlands.* Displayed concentrations of the top 70 cm.

Location	Farm type	management	Treatment	Field size ha	mineral top layer thickness m	schalter present	thickness peat layer m	Organic matter % *	Carbon content kg C-m^2-70cm	C:N*
A	Organic	Grazing	SSI	2	0.40	-	1.6	38.6	53.4	29.2
			Control	0.6	0.35	-	2.0	26.8	47	19.8
B	Conventional	Grazing	SSI	2.3	-	-	1.4	76.8	68.1	34.6
			Control	2.3	-	-	1.4	80.6	74.9	32.8
C	Conventional	Mowing	SSI	1.2	0.30	yes	1.3	47.9	56.3	23
			Control	1.8	0.30	yes	1.0	50.4	60.5	23.5
D	Conventional	Mowing	SSI	2.4	0.30	yes	0.9	37.5	59.6	23.3
			Control	3.5	0.25	yes	0.9	60.8	63.4	26.9

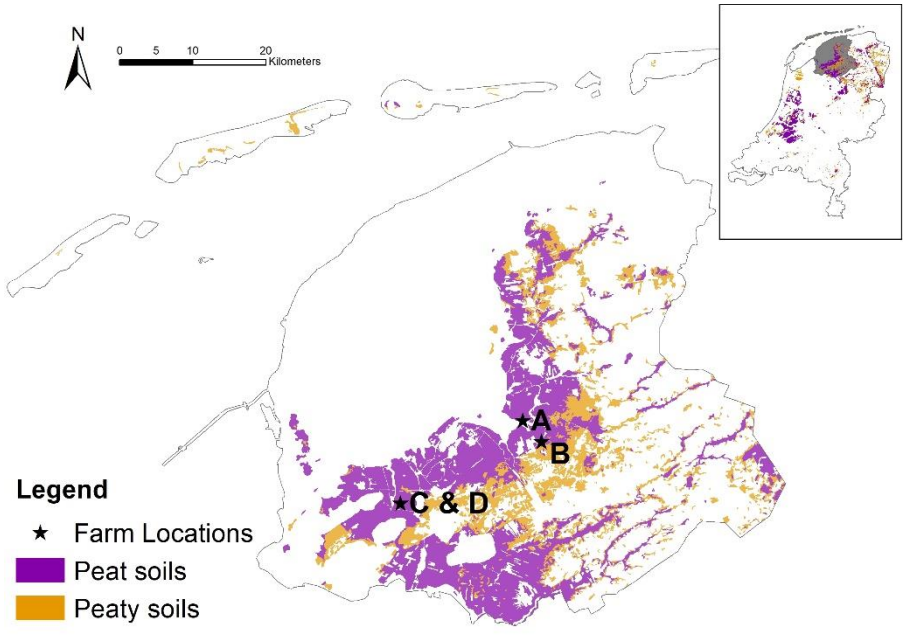

Figure 1 Field locations situated in the province of Friesland, with soil types. Peat soils refer to soils with an organic layer of at least 40 cm within the first 120 cm, while peaty soils are soils with an organic layer of 5-40 cm within the first 80 cm. Insert shows these soil types in the Netherlands, with the location of the field locations in grey.

https://doi.org/10.5194/bg-2020-230
Preprint. Discussion started: 2 July 2020

2.2 Experiment setup

Four sites were set up at dairy farms with land management and soil types representative for Friesland (see Table 1 and Fig. 1). Each location consisted of a treatment site with sub-soil irrigation pipes and a control site. The irrigation pipes were installed at a depth of 70 cm below the surface and 6 m (2,000 m drains ha^{-1}) apart from each other, except for the D location where pipes were 5 m apart. The pipes were either directly connected to the ditch (A and C) or connected to a collection tube before connected into the ditch (B and D). The connections with ditches were placed 10 cm below the maintained ditchwater level. The control sites are fields that have traditional drainage, through a system with deep drainage ditches with convex fields and small shallow ditches.

On the treatment sites, three gas measurement frames in 80x80 cm squares were placed on 0.5 m, 1.5 m and 3 m distance from the chosen irrigation pipe (Fig. 2), representing best the variation in the environmental conditions and vegetation.

Dip well tubes were installed to monitor water levels 0.5, 1.5 and 3 m from the pipe, pairing with the locations of gas measurement frames (Fig. 2). The nylon coated tubes were 5 cm wide and perforated filters placed in the peat layer. The tube 1.5 m from the irrigation pipe was equipped with a pressure sensor and a data logger (ElliTrack-D, Leiderdorp instruments, Leiderdorp, Netherlands) that measures and records the GWT every hour. Ten more dip well tubes were further placed at intervals 0.5 and 3 m from the pipes in the field, which were manually sampled every 2 weeks during gas sampling campaigns, to obtain the variation on field scale.

Soil temperature at -5, -10 and -20 cm depth and soil moisture were continuously measured (12-Bit Temperature sensor -S-TMB-M002 and 10HS Soil Moisture Smart Sensor, Onset Computer Corporation, Bourne, USA) and recorded every 5 min on a data logger (HOBO H21-USB Micro Station Onset Computer Corporation, Bourne, USA). Because of the frequent failure of sensors, extra temperature sensors (HOBO™ pendant loggers, model UA-002-64, Onset Computer Corporation, Bourne, USA) were placed in the soil at a depth of -10 cm.

https://doi.org/10.5194/bg-2020-230
Preprint. Discussion started: 2 July 2020

At farms A and D, sensors were set up at 1.5 m above ground to measure photosynthetically active radiation (PAR, Smart Sensor S-LIA-M003, ONSET Computer Corporation, Bourne, USA), air temperature and air humidity (Temperature/Relative Humidity Smart Sensor, S-THB-M002, Onset Computer Corporation, Bourne, USA). Data were logged every 5 minutes (HOBO H21-USB Micro Station, Onset Computer Corporation, Bourne, USA). Average air temperature and precipitation from the weather station Leeuwarden (18 to 30 km distance from research sites) were used. (KNMI, data). The location specific precipitation was estimated using radar images.

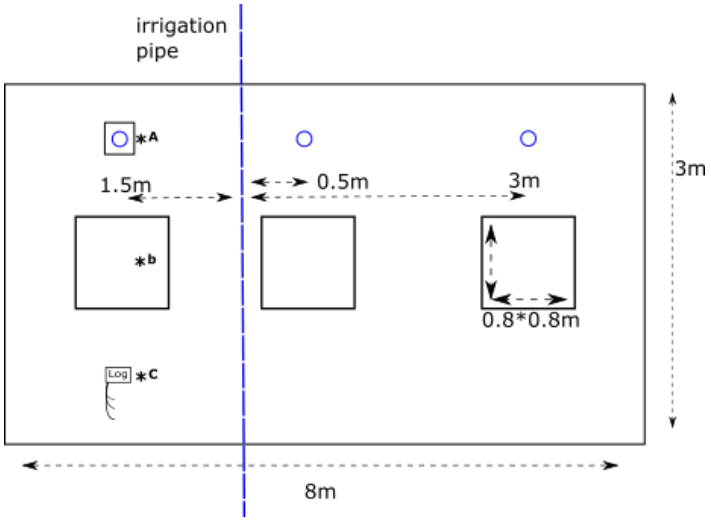

Figure 2 Overview field site SSI. Blue dashed line = irrigation pipe, blue circle = dipwell, A – dipwell with data logger, B – gas measurement frame, C – data logger, -5 -10 -20 soil temperature and soil moisture

The sites were managed with 4-5 cuts per year. Due to grazing disturbance in 2018, an estimation instead of measurements was made for the C-export of location A in consultation with the farmer, but excluded from statistical analysis. Four times per year slurry manure from location C was applied to all plots. The slurry was diluted with ditchwater (2:1 ratio) and applied above ground in the gas measurement frames and the surrounding area. (0.61 kg m^{-2} yr^{-1} dw for 2017 and 0.62 kg m^{-2} yr^{-1} dw for 2018 with a C/N ratio of 16.3±1.3

https://doi.org/10.5194/bg-2020-230
Preprint. Discussion started: 2 July 2020

145 **2.3 Flux measurements**

CO_2 exchange was measured from January 2017 to December 2018, at a frequency of two measurement campaigns a month during growing season (April – October) and once a month during winter. This resulted in 34 (A), 35 (C and D) and 38 (B) campaigns over the two years. A measurement campaign consisted of flux measurements with opaque (dark) and transparent (light) closed chambers (0.8x0.8x0.5 m) to be able to distinguish ecosystem respiration (R_{eco}) and gross primary production
150 (GPP) from net ecosystem exchange (NEE). During winter an average of 9 light and 10 dark measurements, and during summer 18 light and 20 dark measurements were carried out over the course of the day, to achieve data over a gradient in soil temperature and PAR.

The chamber was placed on a frame installed into the soil and connected to a fast greenhouse gas analyzer (GGA) with cavity
155 ring-down spectroscopy (GGA-24EP, Los Gatos Research, Santa Clara, CA, USA) to measure CO_2 and CH_4 or to a G2508 gas concentration analyzer with cavity ring-down spectroscopy (G2508 CRDS Analyzer, Picarro, Santa Clara, CA, USA) to measure N_2O. To prevent heating and to ensure thorough mixing of the air inside the chamber, the chambers where equipped with two fans running continuously during the measurements. For CO_2 and CH_4, each flux measurement lasted on average 180s. N_2O fluxes were measured on all frames at least once during a measurement campaign, with an opaque chamber for
160 480s per flux.

PAR was manually measured (Skye SKP 215 PAR Quantum Sensor, Skye instruments Ltd, Llandrindod Wells, United Kingdom) during the transparent measurements, on top of the chamber. Within each measurement, a variation in PAR higher than 75 µmol m^{-2} s^{-1} would lead to a restart of the measurement. Soil temperature was measured manually in the frame after
165 the dark measurements at -5 and -10 cm depth (Greisinger GTH 175/PT Thermometer, GMH Messtechnik GmbH, Regenstauf, Germany). Crop height was measured before starting the measurement campaign. The biomass was harvested five times per year. These samples where weighed and dried at 70 °C until constant weight. Total nitrogen (TN) and total carbon (TC) was determined in dry plant material (3 mg) using an elemental CNS analyzer (NA 1500, Carlo Erba; Thermo Fisher Scientific, Franklin, USA)

https://doi.org/10.5194/bg-2020-230
Preprint. Discussion started: 2 July 2020

2.4 Data analyses

2.4.1 Flux calculations

Gas fluxes were calculated using the slope of gas concentration over time (Almeida et al., 2016) (eq.1).

$$F = \frac{V}{A} * slope * \frac{P * F1 * F2}{R * T} \quad (1)$$

Where F is gas flux (mg m^2 d^{-1}), V is chamber volume (0.32 m^3), A is the chamber surface area (0.64 m^2), slope is the gas concentration change over time(ppm $second^{-1}$); P is atmospheric pressure (kPa); F1 is the molecular weight, 44 g mol^{-1} for CO_2 and N_2O and 16 g mol^{-1} for CH_4; F2 is the conversion factor of seconds to days; R is gas constant (8.3144 J K^{-1} mol^{-1}); and T is temperature in Kelvin (K) in the chamber.

2.4.2 R_{eco} modeling

To gap-fill for the days that were not measured for an annual balance for CO_2 exchange, R_{eco} and GPP models needed to be fitted with the measured data for each measurement campaign. R_{eco} was fitted with the Lloyd-Taylor function (Lloyd and Taylor, 1994) based on soil temperature (Eq. 2):

$$R_{eco} = R_{eco,Tref} * e^{E_0 * \left(\frac{1}{T_{ref} - T_0} - \frac{1}{T - T_0}\right)} \quad (2)$$

where R_{eco} is ecosystems respiration, $R_{eco,Tref}$ is ecosystem respiration at the reference temperature (T_{ref}) of 281.15 K and was fitted for each measurement campaign, E_0 is long term ecosystem sensitivity coefficient (308.56, (Lloyd and Taylor, 1994)), T_0 Temperature between 0 and T (227.13, Lloyd and Taylor, 1994), T is the observed soil temperature (K) at 5 cm depth and T_{ref} is the reference temperature (283.15 K). If it was not possible to get a significant relationship between the T and the R_{eco} with data from a single campaign, data were pooled for two measuring days to achieve significant fitting (Beetz et al., 2013;Poyda et al., 2016;Karki et al., 2019)

2.4.3 GPP modeling

GPP was obtained by subtracting the measured R_{eco} (CO_2 flux measured with the dark chambers) from the measured NEE (CO_2 flux measured with the light chambers). For the days in between the measurement campaigns, data were modeled with

https://doi.org/10.5194/bg-2020-230
Preprint. Discussion started: 2 July 2020

the relationship between the GPP and PAR using a Michaelis–Menten light optimizing response curve (Kandel et al., 2016;Beetz et al., 2013). For each measurement location per measurement campaign, the GPP was modeled by the parameters α and GPP_{max} (maximum photosynthetic rate with infinite PAR) of (eq.3):

$$NEE = \frac{\alpha * PAR * GPP_{max}}{GPP_{max} + \alpha * PAR} - R_{eco} \quad (3)$$

where NEE is the measured CO_2 flux with light chamber, α is ecosystem quantum yield (mg CO_2 m^{-2} s^{-1}) which is the linear change of GPP per change in PAR at low light intensities (<400 µmol m^{-2} s^{-1} as in (Falge et al., 2001), PAR is measured photosynthetic active radiation (µmol quantum m^{-2} s^{-1}), GPP_{max} is gross primary productivity at its optimum, R_{eco} is ecosystem respiration measured for light response curve and for the year budget calculated with the Lloyd–Tayler function where used. The fitted parameters were linearly interpolated between the measurement campaigns. Due to low coverage of the PAR range in a single measurement campaign in data from year 2017, the complete data set of 2017 were divided into summer and winter periods, and the two datasets (instead of every field campaign) were fitted for the corresponding period per location.

2.4.4 Yearly budget calculations

The calculated parameters were used to interpolate the data for a yearly budget. For the GPP, an important factor of grass growth was added by assuming a linear development of the model parameters α and GPP max, since the plant biomass continued growing between the measurement dates. The NEE year budgets were calculated using the interpolated hourly R_{eco} and GPP values. Extrapolated values at times between two modeled measurements are weighted averages, where the weights are temporal distances of the extrapolated time spots to both of the measurements.

Besides the campaign-wise gap-filling strategy introduced above, other approaches exist to calculate NEE year budget that may result in different values (Karki et al. 2019), which is considered an important source of uncertainty in our study. To quantify this uncertainty, six R_{eco} models and four GPP models were select from Karki et al. (2019) and fitted with annual data (Supplement Table 1). The models with Nash–Sutcliffe modeling efficiencies (NSE) larger than 0.5 (Hoffmann et al. 2015)

https://doi.org/10.5194/bg-2020-230
Preprint. Discussion started: 2 July 2020

was accepted and calculated into gap-filled NEE. Not all sites and years have acceptable models due to large variations of measured fluxes within a year. The remaining NEE values were averaged per site per year and compared with the campaign-wise NEE year budgets as a range of uncertainty.

CH_4 and N_2O fluxes per site and measurement campaign were averaged per day. The annual emissions sums where estimated by linear interpolation between the single measurement dates. Global Warming Potential (GWP) of 34 t CO_2-eq and 298 t CO_2-eq per ton for CH_4 and N_2O was used according to IPCC standards (Myhre et al., 2013) to calculate the yearly GHG balance.

2.5 Statistics

The effect of the treatment on gap-filled annual R_{eco} and GPP, the resulting NEE, the C-export data, CH_4, N_2O exchanges and the combined GHG balance were tested by fitting linear mixed-effects models, with farm location as a random effect. Effectiveness of the random term was tested using the likelihood ratio test method. Significance of the fixed terms was tested via Satterthwaite's degrees of freedom method. The treatment effect was further tested using campaign-wise R_{eco} data. Measured R_{eco} fluxes from SSI and Control were calculated into daily averages and paired per date. The data pairs were grouped based on the GWT differences between SSI and control of the dates. Differences between treatments were then analyzed by linear regression of the R_{eco} flux pairs without interception and testing the null hypothesis 'slope of the regression equals to 1'. All statistical analyses were computed using R version 3.5.3 (Team, 2019) using packages lme4 (Bates et al., 2014), lmerTest (Kuznetsova et al., 2017), sjstats (Lüdecke, 2019), and car (Fox and Weisberg, 2018).

https://doi.org/10.5194/bg-2020-230
Preprint. Discussion started: 2 July 2020

3 Results

3.1 Weather conditions

Mean annual air temperature was 10.3 °C for 2017 and 10.7 °C for 2018, which were higher than the 30-year average of 10.1 °C. The growing season (April–September) in 2017 was slightly cooler with 14.3 °C than the average 14.6 °C, while the temperature during the growing season in 2018 was 1.1 °C warmer than average. Precipitation was slightly higher for 2017 840-951 mm compared to the 30-year average of 840 mm (KMNI data). There was a small period of drought in May and June (see Fig.3). In contrast, 2018 was a dry year with average of 546-611 mm. The year is characterized by a period of extreme drought in the summer, from June to the beginning of August, and precipitation lower than average in the fall and winter.

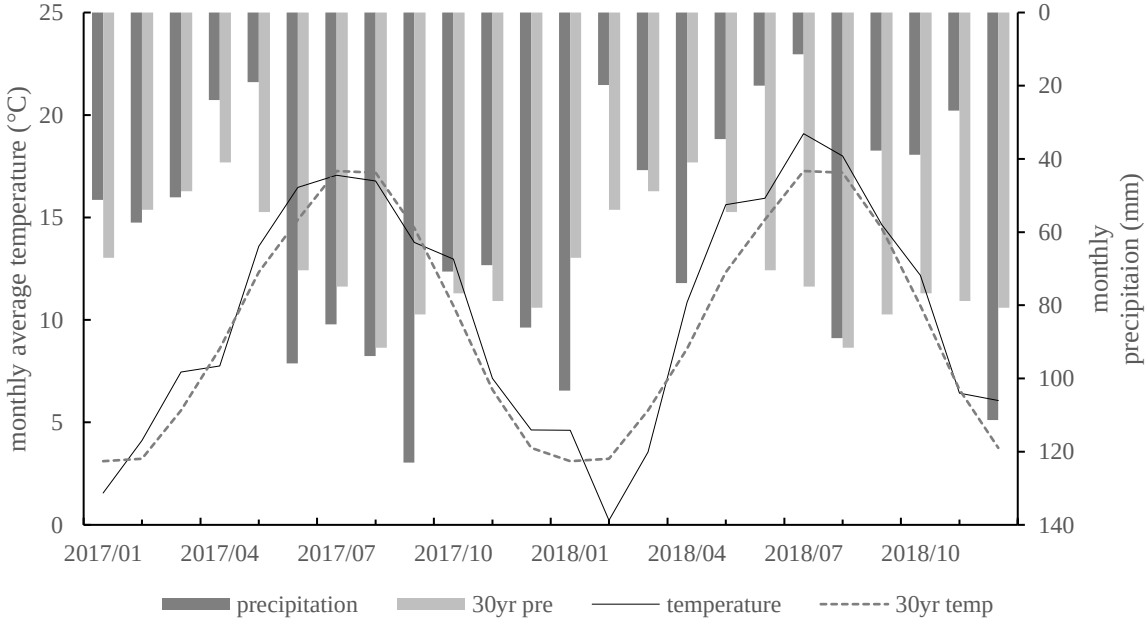

Figure 3 Monthly average air temperature at weather station Leeuwarden (18 to 30 km distance from research sites), and the 30-year average. Sum precipitation at weather station Leeuwarden, and the 30-year average.

https://doi.org/10.5194/bg-2020-230
Preprint. Discussion started: 2 July 2020

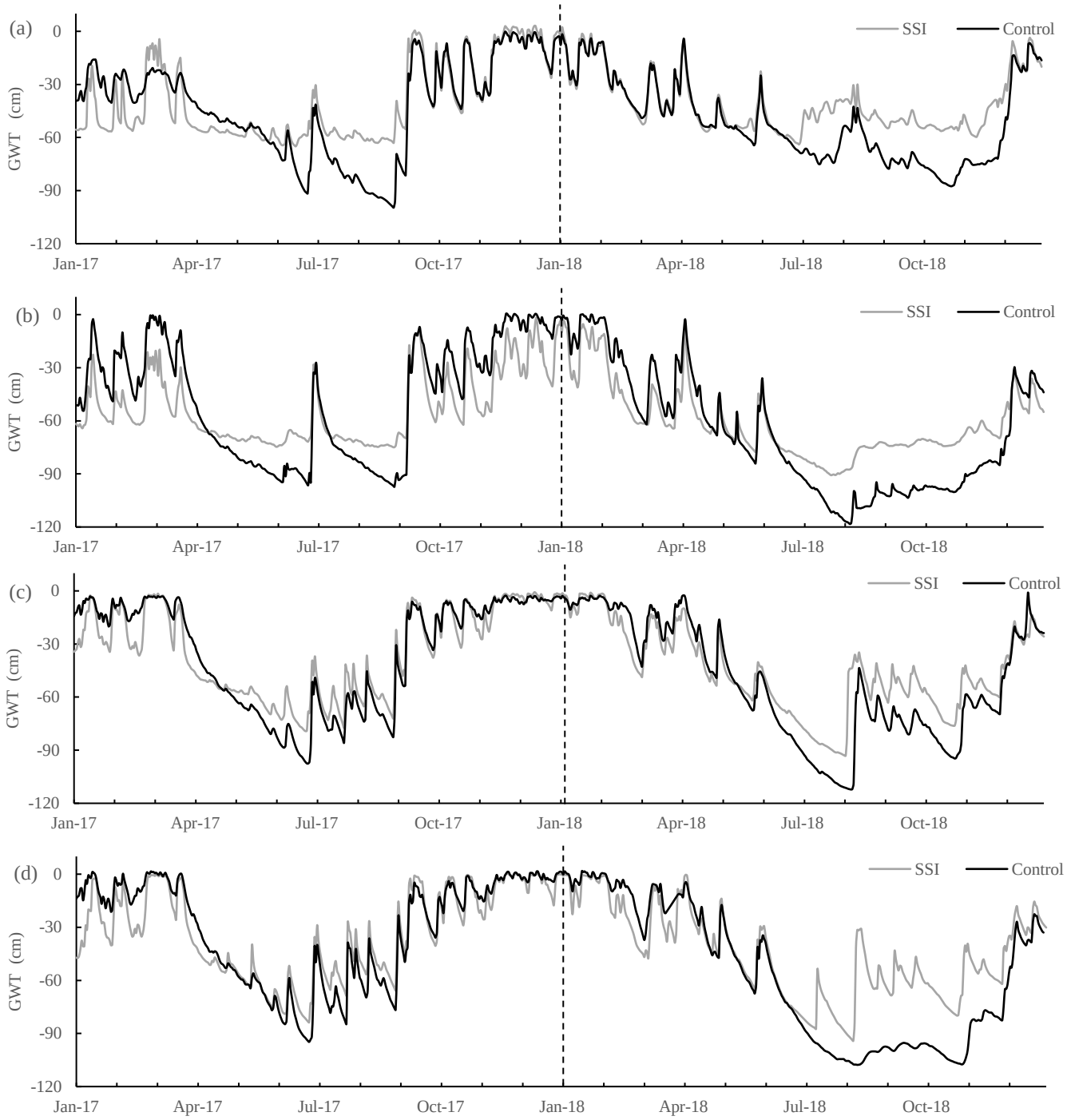

Figure 4 Groundwater table (GWT, below soil surface) during the measuring period per farm (letter), per graph SSI and control.

https://doi.org/10.5194/bg-2020-230
Preprint. Discussion started: 2 July 2020

3.2 Groundwater table (GWT)

Deploying subsurface irrigation (SSI) affected the GWT during the two years for all farms (Fig. 4). However, there was a large variation in effect-size between years and locations. The effect of SSI can be divided into two types of periods. Periods with drainage, in the wet periods, coincided with the autumn (in 2017) and winter period (2017 and 2018). Irrigation periods, where the SSI leads to a higher water table than control, occurred during spring and summer when the GWT dipped below the ditch water level. In 2017, the effectiveness differed per farm. For locations A and B, GWT was more stable in summer around the -60 and -70 for SSI compared to the control, while locations C and D the GWT fluctuated more like in the control fields. During the dry summer of 2018, in contrast, all locations showed a strong effect of irrigation, especially after the dry period in the beginning of august. In this period the water table recovered quickly while the control lagged behind.

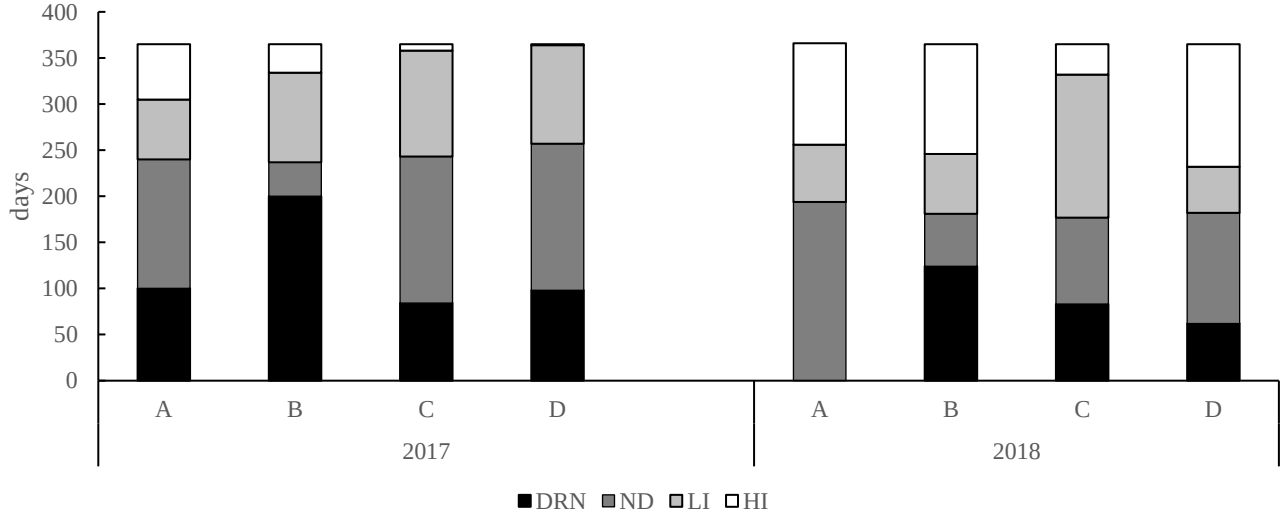

Figure 5 Days with effective drainage/ irrigation for the four locations. DRN, <-5 cm), no difference (ND, -5 ~ 5 cm), low to intermediate irrigation (LI, 5 ~ 20 cm) and high irrigation (HI, > 20 cm)

Although there was hardly any difference in annual average GWT between control and SSI, drainage and irrigation effects could be observed when dividing the calendar year into seasons. The effective days of the SSI are summarized in Fig. 5 according to four categories, based on practical definitions of drainage and irrigation: drainage (DRN, <-5 cm), no difference (ND, -5 ~ 5 cm), low to intermediate irrigation (LI, 5 ~ 20 cm) and high irrigation (HI, > 20 cm). These categories are also used in the statistical analysis of R_{eco} measurements (see 3.7 Seasonal R_{eco}). In 2017 there were 17 days more without any

https://doi.org/10.5194/bg-2020-230
Preprint. Discussion started: 2 July 2020

GWT difference than in 2018. There was a much stronger irrigation effect in the dry year of 2018, with 61 more irrigated days comparing to 2017, and the number of irrigation days was constantly similar to, or higher than the number of drainage days, except for site B in 2017 which had a long period showing a drainage effect.

3.3 Measured R_{eco}

Despite these observed differences in GWT, there was no overall effect of SSI on the total C budget. Comparing days and locations where the R_{eco} was measured with the measured the GWT, provide insight of the effect of SSI. There is variation between emission rates depending on temperature and grass height, but these differences were small during the measurement day due to the regular harvests. However, the R_{eco} values for the measurement days can give an indication for the effectivity of the differences in GWT (Fig. 6). The division between the groups was based on the function of the irrigation pipes, the difference of the GWT between SSI and control on the measurement days (similar to the groups used in Fig. 2). There was a slightly higher R_{eco} for SSI during drainage periods when GWT was lower, which compensates for the lower R_{eco} during summer. For moments where there was no GWT difference and those showing moderate irrigation, there was no effect of SSI on R_{eco}. However, when the GWT of the SSI was more than 20cm higher than the control, the emissions of the control where significantly higher than SSI ($p < 0.01$), indicating an effect of the irrigation. However, this effect of the raised GWT was small, even though in some cases the GWT was raised more than 60 cm. Fig. 5 shows how often the different groups of GWT effects occurred. For 2017 the majority of the days were dominated by drainage (increasing R_{eco}), or by no difference or small irrigation resulting in no effect on the R_{eco}. However, the moments with increased irrigation, when there was a reduced R_{eco} effect of SSI were sparse compared to the other dominating periods.

https://doi.org/10.5194/bg-2020-230
Preprint. Discussion started: 2 July 2020

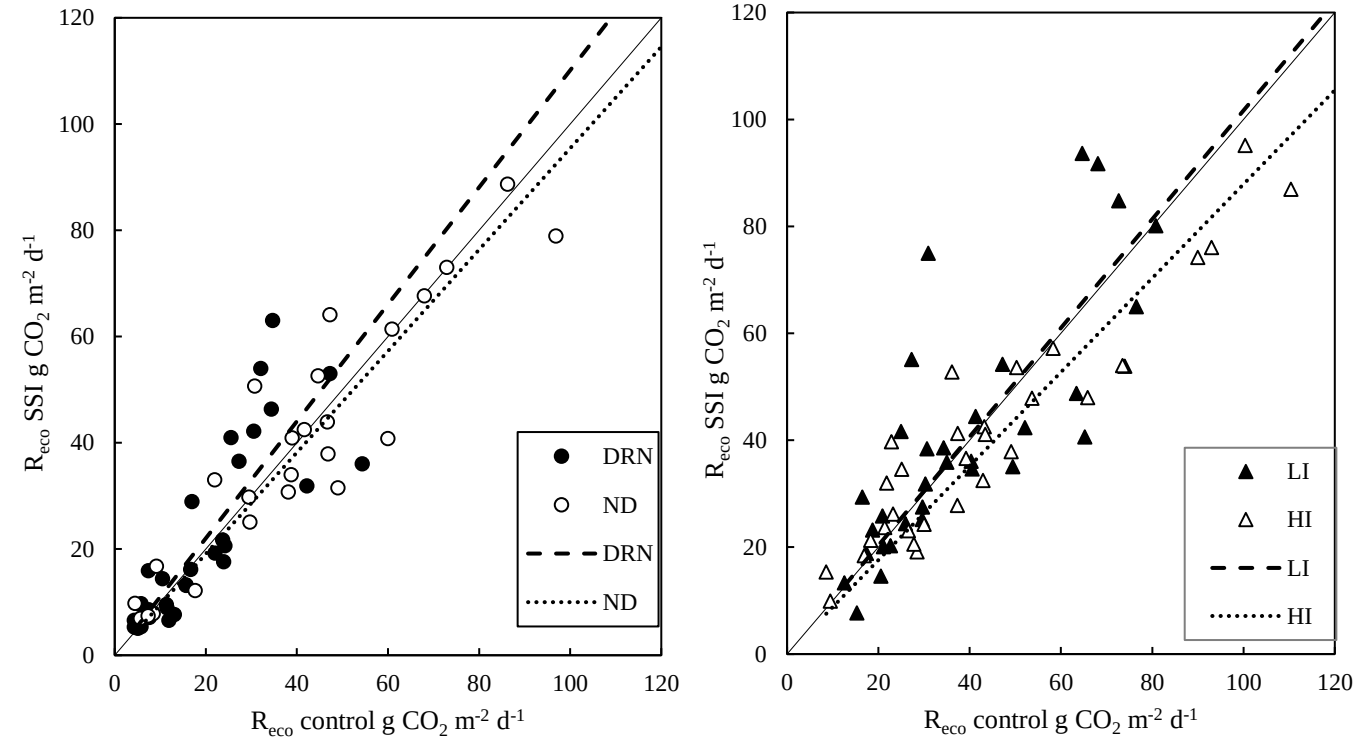

Figure 6 Measured fluxes for ecosystem respiration (R_{eco}), one-to-one comparison in which daily averages where used. a) Values divided into two groups: where the ground water table was lower due to the effect of drainage, and where there was a limited difference. B) Values divided into two groups with irrigation effects, moderate infiltration with more than 5–20 cm difference and high infiltration with more than 20cm difference between SSI and Control. Black filled line is the 1:1 line.

3.4 Annual carbon exchange rates

3.4.1 Gross primary production (GPP)

GPP was high for all locations in both years, showing a clear seasonal pattern with the highest uptake at the start of the summer (Fig.7). GPP was 30% lower in the dry year 2018 ($p < 0.001$) compared to 2017 (see Table 2) and differed between locations (random effect $p = 0.009$). The average GPP over all location for the SSI treatment was -80±4 t CO_2 ha^{-1} yr^{-1} for 2017, and -58±4 t CO_2 eq. ha^{-1} yr^{-1} for 2018. There was, however, no treatment effect on GPP ($p = 0.733$). Average GPP values for all control and SSI plots were -81±4 t CO_2 eq. ha^{-1} yr^{-1} and -80±4 t CO_2 eq. ha^{-1} yr^{-1} for 2017, -55±3 t CO_2 eq. ha^{-1} yr^{-1} and -58±4 t CO_2 eq. ha^{-1} yr^{-1} for 2018, respectively.

https://doi.org/10.5194/bg-2020-230
Preprint. Discussion started: 2 July 2020

3.4.2 Ecosystem respiration (R_{eco})

315 R_{eco} was generally high for all the farms measured during the two years, with the average R_{eco} of 131±1 t CO_2 ha^{-1} yr^{-1} for 2017 being significantly higher than 101±4 t CO_2 ha^{-1} yr^{-1} for 2018 ($p < 0.001$) (Table 2). However, no effect of SSI on R_{eco} was found ($p = 0.350$), with no difference among farm locations (random effect $p = 0.627$). R_{eco} showed a strong seasonal pattern; in 2017 R_{eco} peaked in June and July, while in 2018 the highest R_{eco} was found in May (Fig. 7 Appendix B).

3.4.3 C-export (yield)

320 C-exports (i.e. yields) differed between years without treatment effect of SSI ($p = 0.691$). Following the drought in 2018, C export (13.8±0.6 t CO_2 ha^{-1} yr^{-1}) was significantly lower ($p < 0.001$) than in 2017 (18.0±1.4 t CO_2 ha^{-1} yr^{-1}). These values corresponded to dry matter yields of 9.4±0.6 t DM ha^{-1} yr-1 in 2018 and 12.6±1.1 t DM ha^{-1} yr-^{1} in 2017. The year-effect differed per location (random effect $p < 0.001$). We found a solid relationship between C-export and GPP ($p < 0.001$, $r^2 = 0.942$; linear-mixed modeling).

325 ### 3.4.4 Net ecosystem exchange (NEE)

All locations functioned as large C sources during the measurement period. The annual NEE of all sites and years amounted, on average, to 47.1 t CO_2 ha^{-1} yr^{-1}, with an uncertainty of 3-16 t CO_2 ha^{-1} yr^{-1}. The overall explanatory power of year, treatment and location was low (conditional $r^2 = 0.531$ for fixed and random effects combined) after combining R_{eco} and GPP into NEE. There was, again, no treatment effect of SSI ($p = 0.329$), but there were small differences between both years ($p = 0.040$). NEE
330 values were 67.9±1.6 t CO_2 ha^{-1} yr^{-1} in 2017 and 56.4±5.1 t CO_2 ha^{-1} yr^{-1} in 2018 for the treatment plots. No differences between locations were observed (random effect $p = 0.076$). On average, for all sites and both years, the emission was 62 t CO_2 eq. ha^{-1} yr^{-1} with an uncertainty of 3–16 t CO_2 ha^{-1} yr^{-1}

3.5 Methane exchange

The total exchange of CH_4 was very low during both years. During most periods, the locations functioned as a sink of CH_4.
335 The annual fluxes were -0.01±0.01 t CO_2 eq. ha^{-1} yr^{-1} (-0.25 kg CH_4 ha^{-1} yr^{-1}) for 2017 and -0.06±0.05 t CO_2 eq. ha^{-1} yr^{-1} (-1.8 kg CH_4 ha^{-1} yr^{-1}) for 2018 (table 3). Such exchange did not play a significant part in the total GHG balance (less than 0.4% of

https://doi.org/10.5194/bg-2020-230
Preprint. Discussion started: 2 July 2020

the annual GHG balance), and was not influenced by SSI (p = 0.232) or farm location (random effect p = 0.726). Fluxes only differed between years (p = 0.027).

3.6 Nitrous oxide exchange

The fluxes for N_2O showed a high spatial variability between (random effect p = 0.010) and within all locations, and showed an erratic pattern with mostly low emissions with some high peaks. The highest emissions were measured on the frame closest to the irrigation pipe in the treatment plot of location D, with 4.4 t CO_2 eq. ha^{-1} yr^{-1} for 2017 and 4.9 t CO_2 eq. ha^{-1} yr^{-1} for 2018. The highest peak was measured in August for SSI of location D, showing 55±15 mg N_2O m^{-2} d^{-1}. The peaks observed were erratic, and cannot be explained by year or treatment effect (p = 0.060 and p = 1.000 respectively, marginal r^2 = 0.107 for the fixed effects). Emissions did not correspond to fertilization management with slurry before measurement campaigns.

3.7 Total GHG balance

All sites showed high emissions, without an effect of SSI (p = 0.332) which was consistent for all farms, without location effect (random effect p = 0.099) (table 3). However, there was a large difference between both years, with higher emission rates in 2017 amounting to 63±2 t CO_2 eq. ha^{-1} yr^{-1}, compared 52±3 t CO_2 eq. ha^{-1} yr^{-1} for 2018 ($p<0.001$).

https://doi.org/10.5194/bg-2020-230
Preprint. Discussion started: 2 July 2020

Biogeosciences Discussions Open Access EGU

Table 2 Overview of all processes contributing to the carbon balance calculated for both years. Ecosystems respiration (R_{eco}), gross primary production (GPP), net ecosystems exchange (NEE, sum of GPP and R_{eco}), C-exports from harvest and C-addition from manure for subsoil irrigation (SSI) and control plots at farm locations A-D.

			Carbon exchange				
Year	Location	treatment	R_{eco} t CO_2 ha^{-1} yr^{-1}	GPP t CO_2 ha^{-1} yr^{-1}	NEE t CO_2 ha^{-1} yr^{-1}	C-export t CO_2 ha^{-1} yr^{-1}	C-manure t CO_2 ha^{-1} yr^{-1}
2017	A	SSI	129.4	-75.2	54.2	16.6	-6.9
		Control	134.1	-79.8	54.3	19.3	-6.9
	B	SSI	133.7	-80.6	53.1	15.3	-5.3
		Control	125.9	-74	51.9	15.5	-5.3
	C	SSI	136.3	-91.4	44.9	22.1	-10.9
		Control	129.3	-92.6	36.7	23.3	-10.9
	D	SSI	134.1	-74.6	59.5	15.7	-9.3
		Control	129.1	-77.4	51.6	16.3	-9.3
2018	A	SSI	98.3	-59.3	39	14	-7.4
		Control	102.8	-63.3	39.5	14	-7.4
	B	SSI	117.5	-60.1	57.4	13.8	-9.3
		Control	112.5	-53.5	59	12.2	-9.3
	C	SSI	109.7	-65.6	44.1	15.7	-9.3
		Control	90	-58.5	31.6	15.8	-9.3
	D	SSI	84.2	-45.2	39	13.4	-9.3
		Control	89.6	-46.8	42.8	12	-9.3

355

https://doi.org/10.5194/bg-2020-230
Preprint. Discussion started: 2 July 2020

Biogeosciences Discussions Open Access EGU

Table 3 All GHG emissions contributing to the total GHG balance for subsoil irrigation (SSI) and controls for the four locations (A-D) for both years. The sum of NEE, C-export and C-manure form the total CO_2 flux. The total GHG balance per year, location and treatment is the sum of CO_2, CH_4 and N_2O fluxes in CO_2 equivalents, using radiative forcing factors of 34 for CH_4 and N_2O 298 according to IPCC standards (Myhre et al., 2013).

			GHG fluxes			
Year	Location	treatment	CO_2 t CO_2 ha^{-1} yr^{-1}	CH_4 t CO_2 ha^{-1} yr^{-1}	N_2O t CO_2 ha^{-1} yr^{-1}	Total balance t CO_2 ha^{-1} yr^{-1}
2017	A	SSI	63.9	-0.01	0.09	**64**
		Control	66.7	-0.05	0.72	**67.3**
	B	SSI	63.1	-0.04	2.95	**66**
		Control	62.1	-0.02	1.73	**63.8**
	C	SSI	56.1	-0.03	1.11	**57.2**
		Control	49.1	0.01	1.36	**50.5**
	D	SSI	66	0.01	4.41	**70.4**
		Control	59.2	0.06	4.03	**63.3**
2018	A	SSI	45.6	-0.05	0.18	**45.7**
		Control	46.1	-0.12	1.01	**47**
	B	SSI	61.9	-0.04	2.34	**64.2**
		Control	61.9	0	5.17	**67.1**
	C	SSI	50.5	-0.11	3.25	**53.7**
		Control	38.1	-0.07	4.35	**42.4**
	D	SSI	43.1	-0.09	6.9	**49.9**
		Control	45.5	0.02	3.11	**48.6**

https://doi.org/10.5194/bg-2020-230
Preprint. Discussion started: 2 July 2020

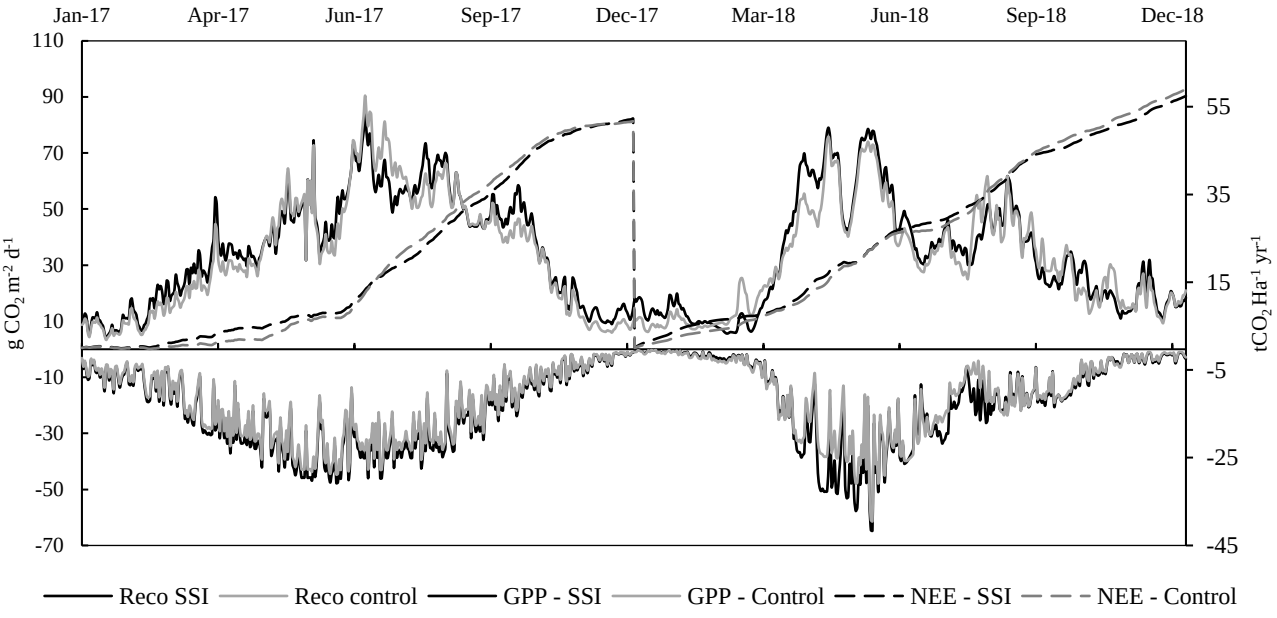

Figure 7 R_{eco} and GPP for location B in g CO_2 m^{-2} d^{-1} on the primary y-axis, for control and SSI. Accumulative NEE in t CO_2 ha^{-1} yr^{-1}, for control and subsoil irrigation (SSI), every year starting at 0.

4 Discussion

For both years, SSI had a clear irrigation effect during summer at the four farms, increasing the GWT on average by 6–18 cm. During winter, there was a moderate but consistent drainage effect, reducing the average GWT in the wet/winter period by 1–20 cm. Despite the irrigation effects and higher water levels in summer, there was no effect of SSI and total GHG balances remained high (62 t CO_2 eq. ha^{-1} yr^{-1} on average of all sites and years with an uncertainty of 3–16 t CO_2 ha^{-1} yr^{-1}). We found no evidence for a reduction of CO_2 emissions, nor for higher yields, on an annual base by implementing SSI.

4.1 SSI does not reduce annual R_{eco}

Despite the higher summer GWT, there was no effect of SSI on the annual R_{eco} at all sites. We found a modest 5–10% reduction in R_{eco} only when GWT differences were larger than 20 cm, based on the direct comparison using raw R_{eco} fluxes (Fig. 6). When the irrigation effect was smaller, no effect on the R_{eco} was found. An earlier study in the Netherlands on the role of GWT also showed small effects of higher summer GWT on R_{eco} and NEE (Net Ecosystem Exchange) despite substantial differences

https://doi.org/10.5194/bg-2020-230
Preprint. Discussion started: 2 July 2020

in soil volume changes/soil subsidence (Dirks et al., 2000). Similarly, the 4-year study (Schrier-Uijl et al., 2014) found little differences in NEE estimates despite substantial large variations in summer GWT and soil moisture contents.

Our findings contradict the general assumption that a higher GWT leads to lower CO_2 emissions, which is often found in near-natural peatlands with the presence of peat-forming vegetation (Wilson et al., 2016a;Lloyd, 2006a;Moore and Dalva, 1993). However, most studies discuss the effect of lower annual average GWT. In addition, there are also studies that did not find an effect of GWT on CO_2 emissions during the season (Parmentier et al., 2009;Lafleur et al., 2005;Nieveen et al., 2005)). This lack of effect is explained by the fact that there is only a small variation in soil moisture values above the GWT. A large number of studies report lower CO_2 emissions when water levels were structurally elevated, concomitant with substantial differences in vegetation/land use following higher water levels (Beetz et al., 2013;Schrier-Uijl et al., 2014;Wilson et al., 2016a). In our study, SSI seems to have an effect of a similar magnitude trending towards higher emissions during periods with lower GWT at the SSI sites.

The small effect size in our study can most probably be explained by differences in peat oxidation rates along the soil profile. Some other studies suggest that the top 30–40 cm layer of the peat profile plays an important role in C turnover rates in drained peatlands, due to more readily decomposable C sources and higher temperatures (Saeurich et al., 2019;Karki et al., 2016;Lafleur et al., 2005;Moore and Dalva, 1993). This soil layer was, however, not affected by higher summer GWTs in our study. Moreover, the top soil layer was even exposed to oxygen for longer periods due to extra drainage during wet seasons. As the infiltrating water will affect the soil moisture content of these layers, it is even expected that this content will approach the optimum for C mineralization more often at the locations where SSI is applied. (Saeurich et al., 2019) speculated that the highest CO_2 production in the top 10 cm is reached when GWTs are approximately 40 cm below the surface (Silvola et al., 1996).

In contrast to surface irrigation where the topsoil is replenished with moisture, the SSI effect is limited to deeper parts of the peat soils, at -60–-100 cm depth. However, the role of this layer as a C source is only limited. Its potency to act as a C source

https://doi.org/10.5194/bg-2020-230
Preprint. Discussion started: 2 July 2020

is reduced by lower temperatures, limited O_2 intrusion, and the fact that water content of this layer is already close to saturation (Taggart et al., 2012;Berglund and Berglund, 2011a;Saeurich et al., 2019). This layer shows low levels of stronger electron acceptors such as O_2 and nitrate used for the microbial oxidation of organic compounds, and of labile organic matter (Fontaine et al., 2007;Leifeld et al., 2012). Visually, the layers deeper than 60 cm are less decomposed (plant macrofossils still visible) compared to the highly degraded uppermost 40 cm.

In addition, lower CO_2 production in the deeper peat layers that are saturated due to the higher water level may be compensated for by the increased CO_2 production in the top 20–40 cm due to the higher moisture levels resulting from elevated water levels. The dry year of 2018 with very low GWT in the control sites (and thus an expected maximized effect of SSI) provides additional evidence that SSI contributes little if any to the mitigation of CO_2 emission from drained peatlands.

4.2 SSI effects on CH_4 and N_2O emissions

Findings of this experiment agree with the generally accepted idea that intensively drained peatlands have low levels of CH_4 emissions, and often these systems even function as a small CH_4 sink (Couwenberg et al., 2011;Couwenberg and Fritz, 2012;Tiemeyer et al., 2016;Maljanen et al., 2010). The SSI site in farm C showed the highest N_2O emissions with 23 kg N_2O $ha^{-1}yr^{-1}$ for 2017. In the current study the average N_2O emission from the drained peatland grasslands was 9 kg N_2O $ha^{-1}yr^{-1}$ falling with the range of annual N_2O emissions from drained peatlands in Northern Europe (4-18 kg N_2O ha^{-1}) (Kandel Tanka et al., 2018;Leahy et al., 2004;Maljanen et al., 2010). Fertilization, temperature and water table fluctuations play major roles in the total N_2O emission (Regina et al., 1999;Van Beek et al., 2011). No distinct peaks were measured after application of fertilizer, and fertilizer was applied on all locations on the same day, so missing peak fluxes would not influence the comparison. The mechanisms of N_2O production and consumption in organic soils are, however, complex and there is high temporal and spatial variability as influenced by site conditions and management (Leppelt et al., 2014;Taghizadeh-Toosi et al., 2019).

https://doi.org/10.5194/bg-2020-230
Preprint. Discussion started: 2 July 2020

4.3 High CO_2 emissions, but lack of effect of SSI on GHG emission

The GPP of the sites (-45.2 – -92.6-80.7 and -56.5 t CO_2 ha^{-1} yr^{-1} in 2017 and 2018, respectively) was in line with values found by (Tiemeyer et al., 2016) for productive and drained peatlands (-70 ± 18 t CO_2 ha^{-1} yr^{-1}) and within the range of grasslands from Europe (45-78 t CO_2 ha^{-1} yr^{-1}) (Eze et al., 2018;Ma et al., 2015;Byrne et al., 2005). The R_{eco} values of the sites (131.5 and 100.6 t CO_2 ha^{-1} yr^{-1} in 2017 and 2018, respectively) are, however, at the higher end of the range (97 ± 33 t CO_2 ha^{-1} yr^{-1} in Tiemeyer et al., 2016). This leads to a relatively high NEE contributing to the generally large annual GHG budgets found in our study. There was, however, a large difference between 2017 and 2018 (-80.7 and -56.5 t CO_2 ha^{-1} yr^{-1}, respectively), which was due to the strong drought effect in 2018. In contrast to our expectations, no effect of SSI was found on GPP. The net GHG budgets from the current study (42.4 – 70.4 t CO_2 eq. ha^{-1} yr^{-1}) fall in the upper range of reported emissions from *drained?* temperate peatlands (Hiraishi et al. 2014, Wilson et al. 2016a). Intensively drained peatlands with productive grassland vegetation tend to emit more CO2 (40–70 t CO_2 ha^{-1} yr^{-1}) (Hoffmann et al., 2015;Tiemeyer et al., 2016;Wilson et al., 2016a;Tiemeyer et al., 2020) than IPCC Tier default values (Hiraishi et al. 2014). Emissions found in the current study were substantially higher than those reported earlier for drained peatlands in the Netherlands (20–25 t CO_2 ha^{-1} yr^{-1} in (Jacobs et al., 2007;Schrier-Uijl et al., 2014). There are a number of reasons for the high emissions found here. Abiotic conditions that favor high CO_2 emissions were present, with high temperatures for both years and optimal moisture conditions for 2017. Research from (Pohl et al., 2015) found a high impact of dynamic soil organic carbon (SOC) and N stocks in the aerobic zone on CO_2 fluxes. In our case, the peat soils contained a high amount of C, especially in the upper 20 cm layer. This layer was also aerobic for long periods during the experiment, thus promoting C formation and transformation processes in the plant–soil system.

4.4 Uncertainties

GHG emissions on peat grasslands are highly variable (Tiemeyer et al., 2016) given the uncertainties from the wide ranges of land use and management activities (Renou-Wilson et al., 2016) and gap filling techniques (Huth et al., 2017). In this study, only uncertainties from gap-filling techniques in terms of data-pooling strategies and model selections were considered.

https://doi.org/10.5194/bg-2020-230
Preprint. Discussion started: 2 July 2020

Campaign-wise fitting of R_{eco} and GPP models can best represent the original data sets, while pooling data for a longer period can provide better model fitness and less bias toward single measurements (Huth et al., 2017;Poyda et al., 2017). However, in this study, different responses of vegetation and soil processes to drought, especially to the extreme drought in 2018, caused abnormal data points that do not fit the classic models, resulting in the generally poor performances of annual models. For this reason, we reported the annual budgets with campaign-wise gap-filled NEE values. The uncertainties of NEE estimates from model differences were on average 14 tons and up to 25 tons of CO_2. Nevertheless, no SSI effect was found considering NEE estimates from annual models. The model differences quantified here were in good agreements with other model tests (Karki et al., 2019;Görres et al., 2014) and match the magnitude of NEE uncertainties calculated with other methods (e.g. the 23–30 tons CO2 variances reported by (Schrier-Uijl et al., 2014) using eddy co-variance techniques).

4.5 Costs and benefits SSI

The intensity of land use (intensity and timing of drainage and fertilization, plant species composition, mowing and grazing regimes) influence the grassland's ability to accumulate or lose C (Renou-Wilson et al., 2016;Smith, 2014;Ward et al., 2016). SSI can increase the load-bearing capacity of the field surface for fertilizing equipment, facilitating earlier fertilization compared to management under current drainage systems. This can also cause increased leaching of water due to earlier drainage in a wet spring. However, the general land-use intensity will not change with the use of SSI. It was expected that C-export via crop yields due to extra drainage could increase in a wet autumn. However, we did not find any indication for an increase in land-use intensity or yield as a result of SSI.

The use of SSI is considered impractical for use in most regions outside of the Netherlands due to the high investment costs for irrigation pipes and the intensive water infrastructure needed for controlling the water level. In addition, irrigation pipes will increase the water demand in summer for these agricultural fields. Both land-use intensity and an increase in yield are related to an increase in CO_2 emissions on drained peat (Beetz et al., 2013;Couwenberg, 2011). The land-use history of our sites favors high CO_2 emission: tillage (cultivators, sod-renewal, and some plowing), cumulative fertilization and well-maintained drainage (Provincie Fryslân ,2015).

https://doi.org/10.5194/bg-2020-230
Preprint. Discussion started: 2 July 2020

5 Main conclusion

Unfortunately, the implementation of SSI does not lead to a reduction of GHG emissions from drained peat meadows, even though there was a clear increase in GWT during summer (especially in the dry year of 2018). We therefore conclude that the use of SSI is ineffective as a mitigation measure to sufficiently lower peat oxidation rates and, therefore, also soil subsidence. Most likely, the largest part of the peat oxidation takes place in the top 70 cm of the soil, which stays above the GWT with the use of SSI. This layer is still exposed to higher temperatures, sufficient moisture, oxygen and alternative electron acceptors such as nitrate, and nutrient input. We expect that SSI may only be effective when the GWT can be raised permanently to levels close to the soil surface (-20–35 cm below the surface).

Data availability. The data are available on request from the corresponding author, (S.T.J. Weideveld).

CRediT authorship contribution statement:

SW: Investigation, Data curation, Writing – original draft, Visualization, Methodology. WL: Investigation, Data curation, Writing – original draft, Visualization. MB: Data curation, Writing – original draft, Visualization. LL: Writing - review & editing, Supervision.CZ: Conceptualization, Methodology, Writing - original draft, Supervision

Acknowledgements

We would like to thank all technical staff, students and others who helped in the field and in the laboratory, as well as the land owners who granted access to the measurement sites. We acknowledge Peter Cruijsen and Roy Peters for their assistance in practical work and analyses. Weier Liu is supported by the China Scholarship Council.

https://doi.org/10.5194/bg-2020-230
Preprint. Discussion started: 2 July 2020

Appendix A annual-models

Table A1. Model selected for annual-model gap-filling approach of year budgets (adopted from Karki et al. 2019).

Model		Structure	Description
R_{eco}	1	$Reco_{T_{ref}} * e^{E_0 * \left(\frac{1}{T_{ref}-T_0}-\frac{1}{T-T_0}\right)}$	Arrhenius function as used for the campaign-wise model fit. Parameters follow descriptions in Material and Methods.
	2	$(Reco_{T_{ref}} + (\alpha * GH)) * e^{E_0 * \left(\frac{1}{T_{ref}-T_0}-\frac{1}{T-T_0}\right)}$	Model 1 adding GH (grass height) as a vegetation factor. α is a scaling parameter of GH.
	3	$Reco_{T_{ref}} * e^{E_0 * \left(\frac{1}{T_{ref}-T_0}-\frac{1}{T-T_0}\right)} + (\alpha * GH)$	Different form of vegetation included Model 1.
	4	$R_0 * e^{bT}$	Exponential function. R_0 is respiration at 0 °C, b is a temperature sensitivity parameter.
	5	$(R_0 + (\alpha * GH)) * e^{bT}$	Model 4 with vegetation included.
	6	$R_0 + (b * T) + (\alpha * GH)$	Linear function.
GPP	1	$\frac{\alpha * PAR * GPP_{max}}{GPP_{max} + \alpha * PAR}$	Michaelis-Menten light response curve as used for the campaign-wise model fitting.
	2	$\frac{\alpha * PAR * GPP_{max} * GH}{GPP_{max} * GH + \alpha * PAR} * FT$	Model 1 with vegetation and air temperature included. FT is a temperature dependent function of photosynthesis set to 0 below - 2 °C and 1 above 10 °C and

https://doi.org/10.5194/bg-2020-230
Preprint. Discussion started: 2 July 2020

			with an exponential increase between - 2 and 10 °C.
	3	$\frac{GPP_{max} * PAR}{\kappa + PAR} * (\frac{GH}{GH + a})$	Another form of the Michaelis-Menten light response curve with a vegetation term included. a is a model-specific parameter.
	4	$\frac{GPP_{max} * PAR}{\kappa + PAR} * \left(\frac{GH}{GH + a}\right) * FT$	Model 3 with air temperature included.

495

https://doi.org/10.5194/bg-2020-230
Preprint. Discussion started: 2 July 2020

Appendix B Reco ,GPP and NEE

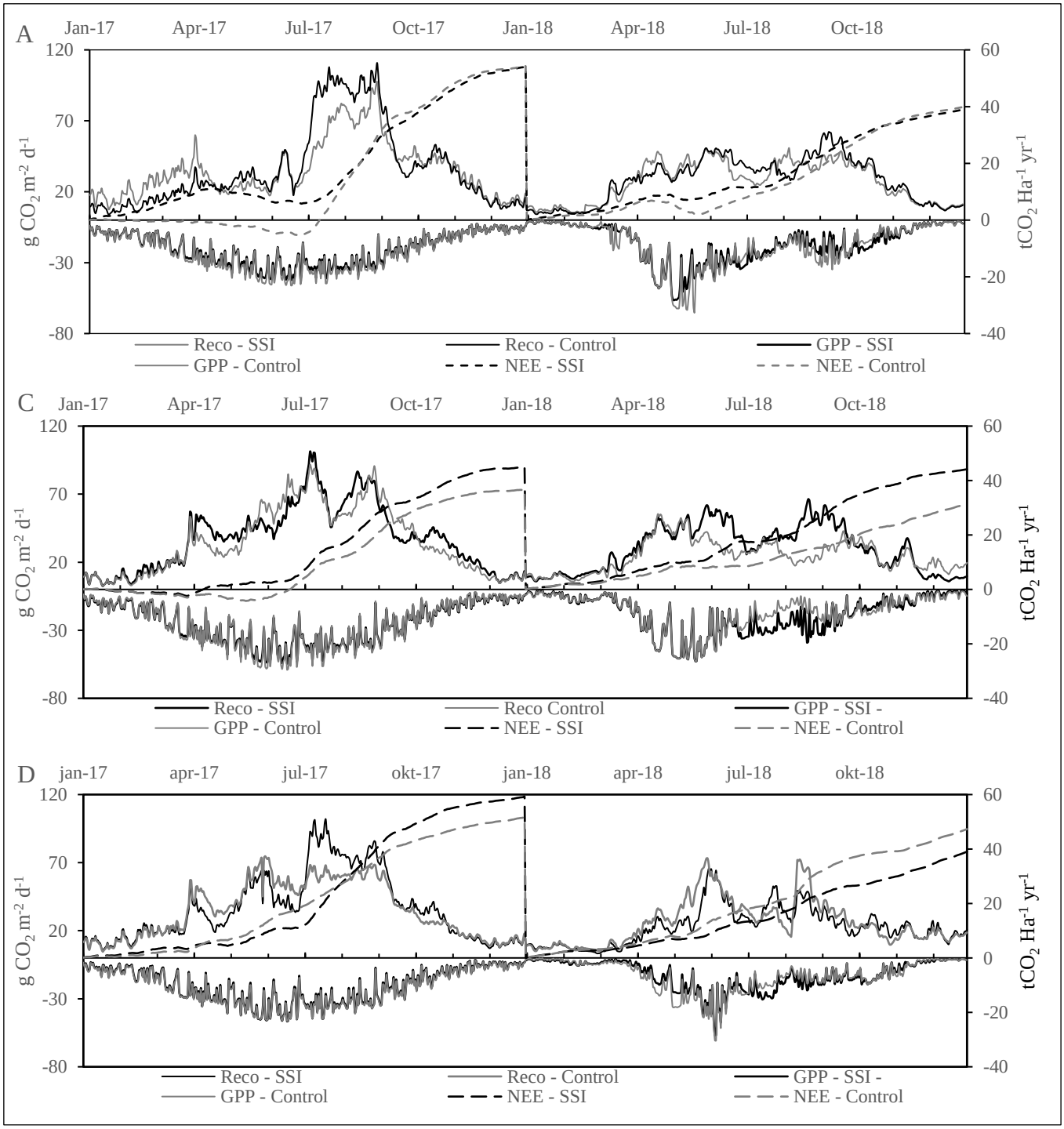

Figure B1 Daily R_{eco} and GPP for location in g CO2 *m-1 d-1* on the primary y-axis, for control and SSI for location Ger. Accumulative NEE in tCO2 Ha-1 yr-1, for control and SSI, every year starting at 0.

https://doi.org/10.5194/bg-2020-230
Preprint. Discussion started: 2 July 2020

Biogeosciences Discussions Open Access EGU

Appendix C N_2O exchange

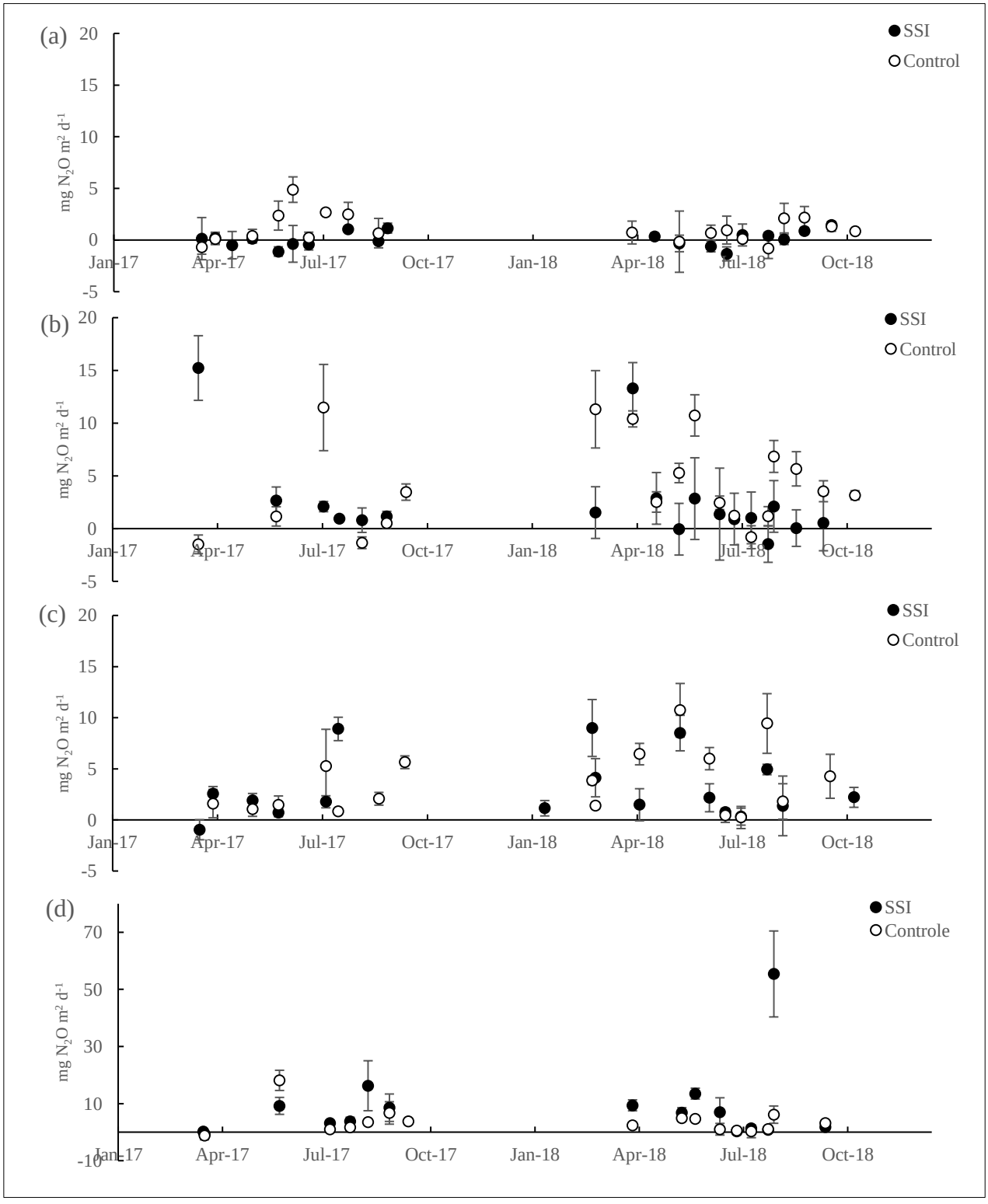

Figure C1 N_2O exchange throughout 2017 and 2018 in mg N_2O m^{-2} d^{-1}.

https://doi.org/10.5194/bg-2020-230
Preprint. Discussion started: 2 July 2020

References

Almeida, R. M., Nóbrega, G. N., Junger, P. C., Figueiredo, A. V., Andrade, A. S., de Moura, C. G., Tonetta, D., Oliveira Jr, E. S., Araújo, F., and Rust, F.: High primary production contrasts with intense carbon emission in a eutrophic tropical reservoir, Frontiers in microbiology, 7, 717, 2016.

Bates, D., Mächler, M., Bolker, B., and Walker, S.: Fitting linear mixed-effects models using lme4, arXiv preprint arXiv:1406.5823, 2014.

Beetz, S., Liebersbach, H., Glatzel, S., Jurasinski, G., Buczko, U., and Höper, H.: Effects of land use intensity on the full greenhouse gas balance in an Atlantic peat bog, Biogeosciences, 10, 1067-1082, 2013.

Berglund, O., and Berglund, K.: Influence of water table level and soil properties on emissions of greenhouse gases from cultivated peat soil, Soil Biology and Biochemistry, 43, 923-931, 2011a.

Berglund, Ö., and Berglund, K.: Influence of water table level and soil properties on emissions of greenhouse gases from cultivated peat soil, Soil Biology and Biochemistry, 43, 923-931, 2011b.

Couwenberg, J.: Emission factors for managed peat soils: an analysis of IPCC default values, Emission factors for managed peat soils: an analysis of IPCC default values., 2009.

Couwenberg, J.: Greenhouse gas emissions from managed peat soils: is the IPCC reporting guidance realistic?, Mires & Peat, 8, 2011.

Couwenberg, J., Thiele, A., Tanneberger, F., Augustin, J., Bärisch, S., Dubovik, D., Liashchynskaya, N., Michaelis, D., Minke, M., and Skuratovich, A.: Assessing greenhouse gas emissions from peatlands using vegetation as a proxy, Hydrobiologia, 674, 67-89, 2011.

Couwenberg, J., and Fritz, C.: Towards developing IPCC methane 'emission factors' for peatlands (organic soils), Mires and Peat, 10, 1-17, 2012.

Dawson, Q., Kechavarzi, C., Leeds-Harrison, P., and Burton, R.: Subsidence and degradation of agricultural peatlands in the Fenlands of Norfolk, UK, Geoderma, 154, 181-187, 2010.

Dirks, B., Hensen, A., and Goudriaan, J.: Effect of drainage on CO2 exchange patterns in an intensively managed peat pasture, Climate Research, 14, 57-63, 2000.

Erkens, G., van der Meulen, M. J., and Middelkoop, H.: Double trouble: subsidence and CO 2 respiration due to 1,000 years of Dutch coastal peatlands cultivation, Hydrogeology Journal, 24, 551-568, 2016.

Falge, E., Baldocchi, D., Olson, R., Anthoni, P., Aubinet, M., Bernhofer, C., Burba, G., Ceulemans, R., Clement, R., and Dolman, H.: Gap filling strategies for long term energy flux data sets, Agricultural and Forest Meteorology, 107, 71-77, 2001.

Fontaine, S., Barot, S., Barré, P., Bdioui, N., Mary, B., and Rumpel, C.: Stability of organic carbon in deep soil layers controlled by fresh carbon supply, Nature, 450, 277-280, 2007.

Fox, J., and Weisberg, S.: An R companion to applied regression, Sage Publications, 2018.

https://doi.org/10.5194/bg-2020-230
Preprint. Discussion started: 2 July 2020

Gorham, E., Lehman, C., Dyke, A., Clymo, D., and Janssens, J.: Long-term carbon sequestration in North American peatlands, Quaternary Science Reviews, 58, 77-82, 2012.

Görres, C.-M., Kutzbach, L., and Elsgaard, L.: Comparative modeling of annual CO2 flux of temperate peat soils under permanent grassland management, Agriculture, ecosystems & environment, 186, 64-76, 2014.

Hartman, A., Schouwenaars, J., and Moustafa, A.: De kosten voor het waterbeheer in het veenweidegebied van Friesland, H 2 O, 45, 25, 2012.

Hendriks, D., Van Huissteden, J., Dolman, A., and Van der Molen, M.: The full greenhouse gas balance of an abandoned peat meadow, 2007a.

Hendriks, R., Wollewinkel, R., and Van den Akker, J.: Predicting soil subsidence and greenhouse gas emission in peat soils depending on water management with the SWAP-ANIMO model, Proceedings of the First International Symposium on Carbon in Peatlands, Wageningen, The Netherlands, 15-18 April 2007, 2007b, 583-586,

Herbert, E. R., Boon, P., Burgin, A. J., Neubauer, S. C., Franklin, R. B., Ardón, M., Hopfensperger, K. N., Lamers, L. P., and Gell, P.: A global perspective on wetland salinization: ecological consequences of a growing threat to freshwater wetlands, Ecosphere, 6, 1-43, 2015.

Hoogland, T., Van den Akker, J., and Brus, D.: Modeling the subsidence of peat soils in the Dutch coastal area, Geoderma, 171, 92-97, 2012.

Hooijer, A., Page, S., Canadell, J., Silvius, M., Kwadijk, J., Wosten, H., and Jauhiainen, J.: Current and future CO2 emissions from drained peatlands in Southeast Asia, Biogeosciences, 2010.

Hoving, I., Massop, H., van Houwelingen, K., van den Akker, J., and Kollen, J.: Hydrologische en landbouwkundige effecten toepassing onderwaterdrains in polder Zeevang: vervolgonderzoek gericht op de toepassing van een zomer-en winterpeil, Wageningen UR Livestock Research1570-8616, 2015.

Huth, V., Vaidya, S., Hoffmann, M., Jurisch, N., Günther, A., Gundlach, L., Hagemann, U., Elsgaard, L., and Augustin, J.: Divergent NEE balances from manual-chamber CO2 fluxes linked to different measurement and gap-filling strategies: A source for uncertainty of estimated terrestrial C sources and sinks?, Journal of Plant Nutrition and Soil Science, 180, 302-315, 2017.

Joosten, H., and Clarke, D.: Wise use of mires and peatlands: background and principles including a framework for decision-making, International Mire Conservation Group, 2002.

Joosten, H.: The Global Peatland CO2 Picture: peatland status and drainage related emissions in all countries of the world, The Global Peatland CO2 Picture: peatland status and drainage related emissions in all countries of the world., 2009.

Jurasinski, G., Glatzel, S., Hahn, J., Koch, S., Koch, M., and Koebsch, F.: Turn on, fade out-methane exchange in a coastal fen over a period of six years after rewetting, EGU General Assembly Conference Abstracts, 2016,

Kabat, P., Fresco, L. O., Stive, M. J., Veerman, C. P., Van Alphen, J. S., Parmet, B. W., Hazeleger, W., and Katsman, C. A.: Dutch coasts in transition, Nature Geoscience, 2, 450-452, 2009.

https://doi.org/10.5194/bg-2020-230
Preprint. Discussion started: 2 July 2020

Kandel Tanka, P., Laerke, P. E., and Elsgaard, L.: Annual emissions of CO2, CH4 and N2O from a temperate peat bog: Comparison of an undrained and four drained sites under permanent grass and arable crop rotations with cereals and potato, Agricultural and Forest Meteorology, 256, 470-481, 2018.

Kandel, T. P., Lærke, P. E., and Elsgaard, L.: Effect of chamber enclosure time on soil respiration flux: A comparison of linear and non-linear flux calculation methods, Atmospheric environment, 141, 245-254, 2016.

Karki, S., Elsgaard, L., Kandel, T. P., and Lærke, P. E.: Carbon balance of rewetted and drained peat soils used for biomass production: a mesocosm study, Gcb Bioenergy, 8, 969-980, 2016.

Karki, S., Kandel, T., Elsgaard, L., Labouriau, R., and Lærke, P.: Annual CO 2 fluxes from a cultivated fen with perennial grasses during two initial years of rewetting, Mires & Peat, 25, 2019.

Kechavarzi, C., Dawson, Q., Leeds-Harrison, P., Szatyłowicz, J., and Gnatowski, T.: Water-table management in lowland UK peat soils and its potential impact on CO2 emission, Soil use and management, 23, 359-367, 2007.

Kuznetsova, A., Brockhoff, P. B., and Christensen, R. H. B.: lmerTest package: tests in linear mixed effects models, Journal of Statistical Software, 82, 2017.

Lafleur, P., Moore, T. R., Roulet, N. T., and Frolking, S.: Ecosystem respiration in a cool temperate bog depends on peat temperature but not water table, Ecosystems, 8, 619-629, 2005.

Lamers, L. P., Vile, M. A., Grootjans, A. P., Acreman, M. C., van Diggelen, R., Evans, M. G., Richardson, C. J., Rochefort, L., Kooijman, A. M., and Roelofs, J. G.: Ecological restoration of rich fens in Europe and North America: from trial and error to an evidence-based approach, Biological Reviews, 90, 182-203, 2015.

Leahy, P., Kiely, G., and Scanlon, T. M.: Managed grasslands: A greenhouse gas sink or source?, Geophysical Research Letters, 31, 2004.

Leifeld, J., Steffens, M., and Galego-Sala, A.: Sensitivity of peatland carbon loss to organic matter quality, Geophysical Research Letters, 39, 2012.

Leifeld, J., and Menichetti, L.: The underappreciated potential of peatlands in global climate change mitigation strategies, Nature communications, 9, 1-7, 2018.

Leppelt, T., Dechow, R., Gebbert, S., Freibauer, A., and Lohila, A.: Nitrous oxide emission budgets and land-use-driven hotspots for organic soils in Europe, Biogeosciences, 11, 6595-6612, 2014.

Lloyd, C.: Annual carbon balance of a managed wetland meadow in the Somerset Levels, UK, Agricultural and Forest Meteorology, 138, 168-179, 2006a.

Lloyd, C. R.: Annual carbon balance of a managed wetland meadow in the Somerset Levels, UK, Agricultural and Forest Meteorology, 138, 168-179, 2006b.

Lloyd, J., and Taylor, J.: On the temperature dependence of soil respiration, Functional ecology, 315-323, 1994.

Lüdecke, D.: sjstats: Statistical Functions for Regression Models (Version 0.17. 4). doi: 10.5281/zenodo. 1284472. 2019.

Maljanen, M., Sigurdsson, B., Guðmundsson, J., Óskarsson, H., Huttunen, J., and Martikainen, P.: Greenhouse gas balances of managed peatlands in the Nordic countries–present knowledge and gaps, Biogeosciences, 7, 2711-2738, 2010.

https://doi.org/10.5194/bg-2020-230
Preprint. Discussion started: 2 July 2020

Moore, T., and Dalva, M.: The influence of temperature and water table position on carbon dioxide and methane emissions from laboratory columns of peatland soils, Journal of Soil Science, 44, 651-664, 1993.

Myhre, G., Shindell, D., Bréon, F., Collins, W., Fuglestvedt, J., Huang, J., Koch, D., Lamarque, J., Lee, D., and Mendoza, B.: Anthropogenic and Natural Radiative Forcing, Climate Change 2013: The Physical Science Basis. Contribution of Working Group I to the Fifth Assessment Report of the Intergovernmental Panel on Climate Change, 659–740. Cambridge: Cambridge University Press, 2013.

Nieveen, J. P., Campbell, D. I., Schipper, L. A., and Blair, I. J.: Carbon exchange of grazed pasture on a drained peat soil, Global Change Biology, 11, 607-618, 2005.

Parmentier, F., Van der Molen, M., De Jeu, R., Hendriks, D., and Dolman, A.: CO2 fluxes and evaporation on a peatland in the Netherlands appear not affected by water table fluctuations, Agricultural and forest meteorology, 149, 1201-1208, 2009.

Poyda, A., Reinsch, T., Kluß, C., Loges, R., and Taube, F.: Greenhouse gas emissions from fen soils used for forage production in northern Germany, Biogeosciences, 13, 5221-5244, 2016.

Poyda, A., Reinsch, T., Skinner, R. H., Kluß, C., Loges, R., and Taube, F.: Comparing chamber and eddy covariance based net ecosystem CO2 exchange of fen soils, Journal of Plant Nutrition and Soil Science, 180, 252-266, 2017.

Regina, K., Silvola, J., and Martikainen, P. J.: Short-term effects of changing water table on N2O fluxes from peat monoliths from natural and drained boreal peatlands, Global Change Biology, 5, 183-189, 1999.

Regina, K., Syväsalo, E., Hannukkala, A., and Esala, M.: Fluxes of N2O from farmed peat soils in Finland, European Journal of Soil Science, 55, 591-599, 2004.

Renou-Wilson, F., Müller, C., Moser, G., and Wilson, D.: To graze or not to graze? Four years greenhouse gas balances and vegetation composition from a drained and a rewetted organic soil under grassland, Agriculture, Ecosystems & Environment, 222, 156-170, 2016.

Saeurich, A., Tiemeyer, B., Dettmann, U., and Don, A.: How do sand addition, soil moisture and nutrient status influence greenhouse gas fluxes from drained organic soils?, Soil Biology and Biochemistry, 135, 71-84, 2019.

Schrier-Uijl, A., Kroon, P., Hendriks, D., Hensen, A., Van Huissteden, J., Berendse, F., and Veenendaal, E.: Agricultural peatlands: towards a greenhouse gas sink-a synthesis of a Dutch landscape study, Biogeosciences, 11, 4559, 2014.

Silvola, J., Alm, J., Ahlholm, U., Nykanen, H., and Martikainen, P. J.: CO_2 fluxes from peat in boreal mires under varying temperature and moisture conditions, Journal of ecology, 219-228, 1996.

Smith, P.: Do grasslands act as a perpetual sink for carbon?, Global change biology, 20, 2708-2711, 2014.

Stephens, J. C., Allen Jr, L., and Chen, E.: Organic soil subsidence, Reviews in Engineering Geology, 6, 107-122, 1984.

Syvitski, J. P., Kettner, A. J., Overeem, I., Hutton, E. W., Hannon, M. T., Brakenridge, G. R., Day, J., Vörösmarty, C., Saito, Y., and Giosan, L.: Sinking deltas due to human activities, Nature Geoscience, 2, 681, 2009.

Taggart, M., Heitman, J. L., Shi, W., and Vepraskas, M.: Temperature and Water Content Effects on Carbon Mineralization for Sapric Soil Material, Wetlands, 32, 939-944, 2012.

https://doi.org/10.5194/bg-2020-230
Preprint. Discussion started: 2 July 2020

Taghizadeh-Toosi, A., Clough, T., Petersen, S. O., and Elsgaard, L.: Nitrous Oxide Dynamics in Agricultural Peat Soil in Response to Availability of Nitrate, Nitrite, and Iron Sulfides, Geomicrobiology Journal, 1-10, 10.1080/01490451.2019.1666192, 2019.

Tanneberger, F., Moen, A., Joosten, H., and Nilsen, N.: The peatland map of Europe, 2017.

Team, R. C.: A language and environment for statistical computing. Vienna, Austria: R Foundation for Statistical Computing; 2012, URL https://www. R-project. org, 2019.

Tiemeyer, B., Albiac Borraz, E., Augustin, J., Bechtold, M., Beetz, S., Beyer, C., Drösler, M., Ebli, M., Eickenscheidt, T., and Fiedler, S.: High emissions of greenhouse gases from grasslands on peat and other organic soils, Global change biology, 22, 4134-4149, 2016.

Tiggeloven, T., De Moel, H., Winsemius, H. C., Eilander, D., Erkens, G., Gebremedhin, E., Loaiza, A. D., Kuzma, S., Luo, T., and Iceland, C.: Global-scale benefit–cost analysis of coastal flood adaptation to different flood risk drivers using structural measures, Nat. Hazards Earth Syst. Sci, 20, 1025-1044, 2020.

Van Beek, C., Pleijter, M., and Kuikman, P.: Nitrous oxide emissions from fertilized and unfertilized grasslands on peat soil, Nutrient cycling in agroecosystems, 89, 453-461, 2011.

Van den Akker, J., Kuikman, P., De Vries, F., Hoving, I., Pleijter, M., Hendriks, R., Wolleswinkel, R., Simões, R., and Kwakernaak, C.: Emission of CO2 from agricultural peat soils in the Netherlands and ways to limit this emission, Proceedings of the 13th International Peat Congress After Wise Use–The Future of Peatlands, Vol. 1 Oral Presentations, Tullamore, Ireland, 8–13 june 2008, 2010, 645-648,

Van den Born, G., Kragt, F., Henkens, D., Rijken, B., Van Bemmel, B., Van der Sluis, S., Polman, N., Bos, E. J., Kuhlman, T., and Kwakernaak, C.: Dalende bodems, stijgende kosten: mogelijke maatregelen tegen veenbodemdaling in het landelijk en stedelijk gebied: beleidsstudie, Planbureau voor de Leefomgeving, 2016.

Van den Bos, R., and van de Plassche, O.: Incubation experiments with undisturbed cores from coastal peatlands (western Netherlands): carbon dioxide fluxes in response to temperature and water-table changes, Human Influence in Carbon Fluxes in Coastal Peatlands; Process Analysis, Quantification and Prediction. PhD thesis, Free University Amsterdam, The Netherlands, 11-34, 2003.

Van Huissteden, J., van den Bos, R., and Alvarez, I. M.: Modelling the effect of water-table management on CO 2 and CH 4 fluxes from peat soils, Netherlands Journal of Geosciences, 85, 3-18, 2006.

Ward, S. E., Smart, S. M., Quirk, H., Tallowin, J. R., Mortimer, S. R., Shiel, R. S., Wilby, A., and Bardgett, R. D.: Legacy effects of grassland management on soil carbon to depth, Global change biology, 22, 2929-2938, 2016.

Wilson, D., Blain, D., Couwenberg, J., Evans, C., Murdiyarso, D., Page, S., Renou-Wilson, F., Rieley, J., Sirin, A., and Strack, M.: Greenhouse gas emission factors associated with rewetting of organic soils, Mires and Peat, 17, 2016a.

Wilson, D., Blain, D., Couwenberg, J., Evans, C. D., and Murdiyarso, D.: Greenhouse gas emission factors associated with rewetting of organic soils, Mires and Peat, 17, 2016b.